Formation of porous metallic glass compacts by electro-discharge sintering

J.Y. Cho[a], J.S. Shin[a], Y.J. Jo[a], J.K. Lee[b], M.H. Lee[c], H.S. Lee[c], W.H. Lee[a], K.B. Kim[a,*]

[a] Department of Advanced Materials Engineering, Sejong University, 98 Gunja-dong, Gwnagjin-gu, 143-747 Seoul, Republic of Korea
[b] Division of Advanced Materials Engineering, Kongju National University, 275 Budae-dong, Seobuk-gu, Cheonan-si, 331-717 Chungnam, Republic of Korea
[c] Advanced Materials Division, Korea Institute of Industrial Technology (KITECH), Dongchon-dong, Yeonsu-gu, 463-130 Incheon, Republic of Korea

ARTICLE INFO

ABSTRACT

A single pulse of 0.1–0.9 kJ/0.45 g atomized amorphous $Cu_{54}Zr_{22}Ti_{18}Ni_6$ powders in size range of 90–150 μm was applied to fabricate porous metallic glass compacts using electro-discharge sintering (EDS) with 3 and 4 mm in diameter. The structural and thermal analysis of the samples indicated that formation of the porous metallic glass compacts occurs only when low electrical input energy was induced on the amorphous powders. Furthermore, the critical input energy inducing crystallization of the amorphous phase during EDS is strongly dependent on the size of the sample.

© 2011 Elsevier B.V. All rights reserved.

1. Introduction

Bulk metallic glasses (BMGs) have much higher strength than conventional crystalline alloys due to their unique atomic structure [1]. Even with such high strength of the BMGs, however, their plasticity at room temperature is considerably limited causing typical catastrophic failure of the sample [2]. Such critical disadvantage of the BMGs often limits the applications of the BMGs as structural materials. In order to overcome the shortage against the engineering applications of the bulk metallic glasses, so far there are several solutions have been suggested [3,4]. Among them, recent development of metallic glass foam has been highlighted due to low specific weight and high energy-absorption capability [5,6]. Furthermore, the dense liquid structure designed to form bulk metallic glasses upon solidification can be a strong merit to enhance the controllability of the pore size, distribution, volume fraction and morphology [6].

In general, typical porous structure, i.e. foam can be classified as either open or closed porous structure. It has been well understood that the open porous structure is mainly utilized for the functional materials including dental, orthopedic and catalytic precursor/performs. In contrast, the closed porous structure is often characterized by the isolated pores to apply for the structural applications. In this scenario, there are several reports on formation of the BMG foam to enhance the plasticity of the BMGs similar to a concept of the BMG composites [7,8]. For example, it has been reported that porous Zr–Cu–Al–Ni metallic glassy alloy fabricated by spark plasma sintering process shows larger plastic ductility and lower Young's modulus than the as-cast specimen [9]. Moreover, the fabrication of the BMG foams often performs based on routine solidification process, i.e. infiltration of the glass-forming liquid on the various preforms, by mixing the melt with hydrated B_2O_3 [10] or holding under pressurized hydrogen [11], etc. However, one can find that the foaming agency such as NaCl preform and hydrogen possibly offering the heterogeneous nucleation sites upon solidification of the glass-forming melt can cause the nucleation of the crystalline phases. In contrast, there are few approaches to fabricate the bulk metallic foam via warm extrusion process combined to selective chemical leaching of the blended fugitive powder [12]. Indeed, it is quite plausible to produce the bulk metallic glass foam containing homogenously distributed directional open pores. However, the warm extrusion process with the selective chemical leaching of the fugitive powder is quite complex and multi-step processing. Hence, it is necessary to develop further efficient processing to fabricate the porous metallic glass compacts.

In the present study, we report the fabrication of porous metallic glass compact having uniformly dispersed pores using electro-discharge sintering (EDS). It has been well known that the EDS is considered as a novel concept to fabricate the porous structure by applying high voltage and high current in times as short as ~300 μs [13,14]. Thus, it is believed that the fabrication of the metastable porous structure such as the metallic glasses without phase transformation is suitable by using the EDS. Furthermore, it is possible to understand that the critical input energy possibly causing the crystallization of the amorphous phase during EDS is

* Corresponding author. Tel.: +82 2 3408 3690; fax: +82 2 3408 3664.
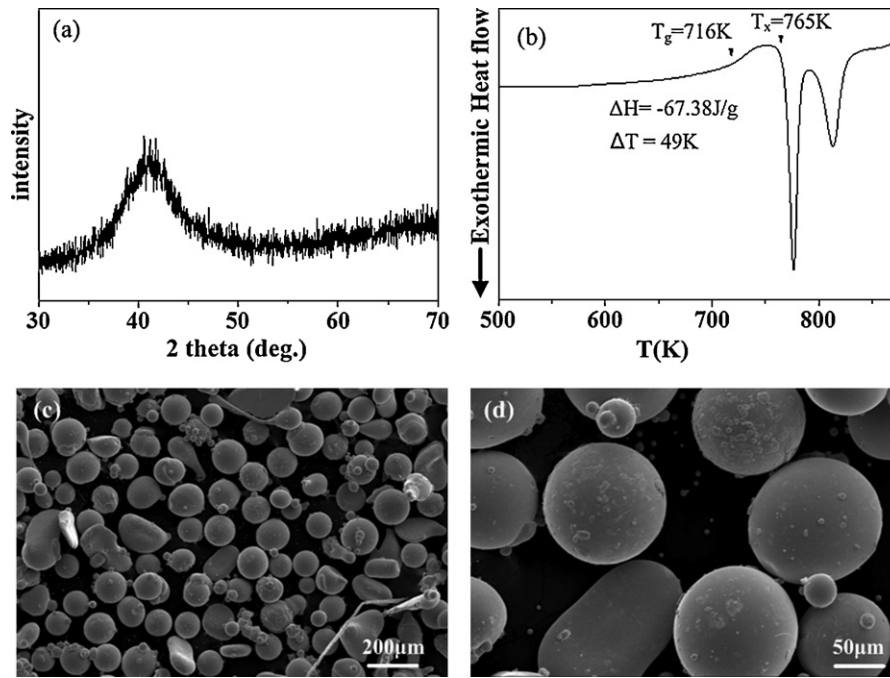E-mail address: kbkim@sejong.ac.kr (K.B. Kim).

Fig. 1. XRD trace (a), DSC trace (b) and SEM secondary electron micrographs [(c) and (d)] of gas-atomized $Cu_{54}Zr_{22}Ti_{18}Ni_6$ powders.

strongly dependent on the size of the porous metallic glass compacts.

2. Experimental procedures

Gas-atomized spherical $Cu_{54}Zr_{22}Ti_{18}Ni_6$ powders in size range of 90–150 μm were weighed by 0.45 g, and then vibration was used to fill the powders into a quartz tube with a diameter of 3.0 and 4.0 mm that had a copper electrode at the bottom. Another copper electrode was placed into the upper quartz tube. The prepared green compact collective was set into the discharging chamber followed by evacuation of 2×10^{-3} Torr. The input energy can be predetermined by controlling input voltage (V) according to the equation:(1)$E = \frac{CV^2}{2}$ where C is the capacitance of a capacitor [15].

One capacitor bank (450 μF) was charged with different electrical input energies (0.1–0.7 kJ). The different input energies were imposed into the prepared green compact collectives by on/off high vacuum switch, which closes the discharge circuit. When the circuit was closed, the voltage and the current take place in the powder column. The overall process is referred to as electro-discharge sintering. More detailed EDS process is described elsewhere [15].

The phase identification for the gas-atomized $Cu_{54}Zr_{22}Ti_{18}Ni_6$ powders and the discharged compacts was done in D/MAX-2500/PC X-ray diffractometer (XRD) using Cu Kα radiation. A differential scanning calorimeter (DSC) was used to analyze the thermal stability of the $Cu_{54}Zr_{22}Ti_{18}Ni_6$ powders under a flowing pure argon atmosphere at a heating rate of 40 K/min. The gas-atomized $Cu_{54}Zr_{22}Ti_{18}Ni_6$ powder and porous metallic glass compacts were examined using scanning microscopy (SEM). Pore size and size distribution were measured by examining SEM images using linear interception method. Micro-Vickers hardness measure-
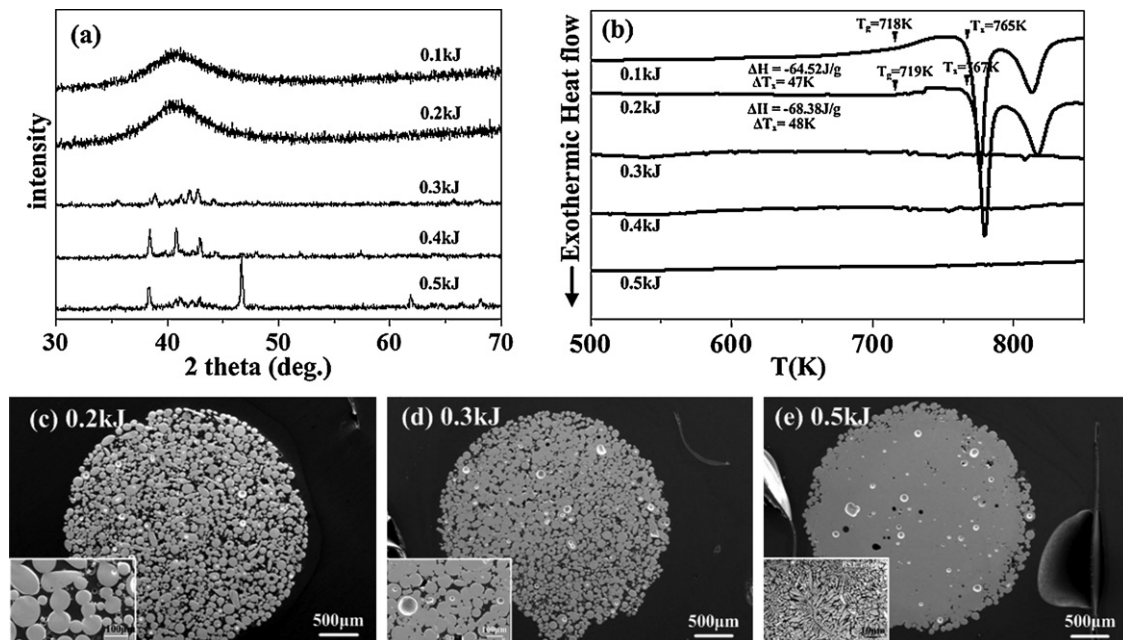

Fig. 2. XRD traces (a), DSC traces (b) and SEM micrographs [(c)–(e)] of the porous $Cu_{54}Zr_{22}Ti_{18}Ni_6$ metallic glass compacts with 3 mm in diameter fabricated using EDS with various electrical input energies (0.1–0.5 kJ).

Fig. 3. XRD traces (a), DSC traces (b) and SEM micrographs [(c)–(e)] of the porous $Cu_{54}Zr_{22}Ti_{18}Ni_{6}$ metallic glass compacts with 4 mm in diameter fabricated using EDS with various electrical input energies (0.3–0.7 kJ).
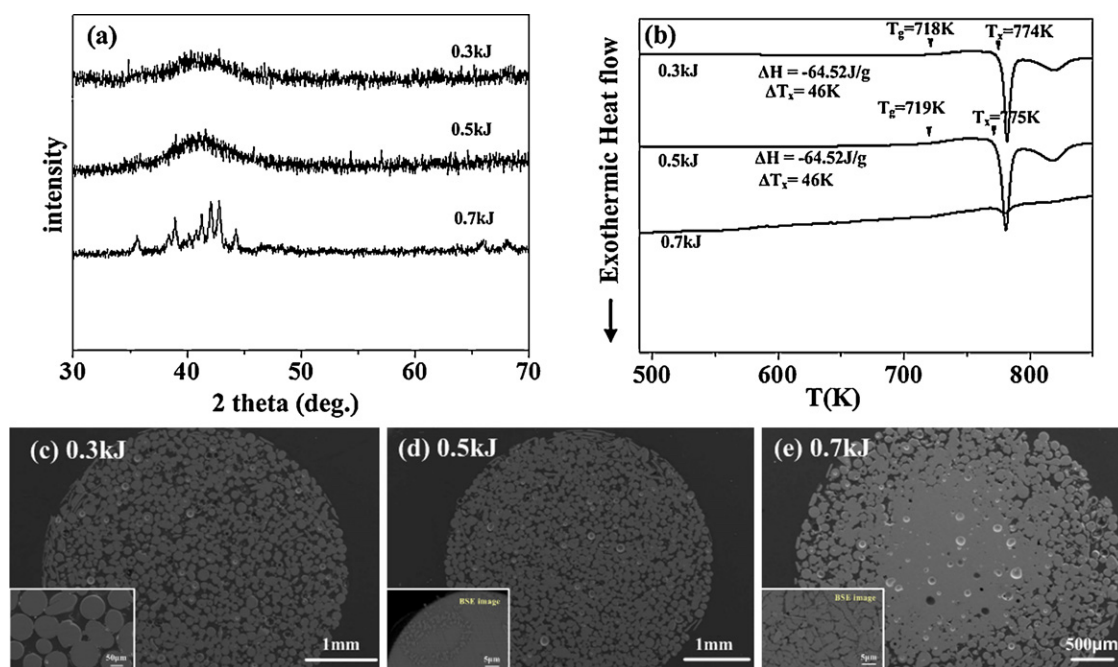
ments were performed for the sample in order to assess the stability of the neck formed.

3. Results and discussion

Fig. 1 shows XRD trace (a), DSC trace (b) and SEM secondary electron micrographs [(c) and (d)] of gas-atomized $Cu_{54}Zr_{22}Ti_{18}Ni_{6}$ powders. The XRD trace in Fig. 1(a) presents broad diffraction maxima representing the typical characteristic of an amorphous structure. The DSC trace exhibits a wide supercooled liquid region, $\Delta T = T_x (= 765\,K) - T_g (= 716\,K) = 49\,K$, where T_x and T_g are the onset temperatures of the crystallization and glass transition events, respectively. The heat release of the exothermic reactions, ΔH, is ~67.38 J/mol. Furthermore, SEM micrographs reveal the spherical morphology of the powders with the smooth surface. The size of the spherical $Cu_{54}Zr_{22}Ti_{18}Ni_{6}$ powders is measured to be 90–150 μm. Hence, it is believed that the spherical amorphous $Cu_{54}Zr_{22}Ti_{18}Ni_{6}$ powders with a size range of 90–150 μm have been successfully fabricated through gas-atomized process.

Fig. 2 shows XRD traces (a), DSC traces (b) and SEM micrographs [(c)–(e)] with inset SEM micrographs obtained at higher magnification of the porous $Cu_{54}Zr_{22}Ti_{18}Ni_{6}$ metallic glass compacts with 3 mm in diameter fabricated using EDS with different electrical input energies (0.1–0.5 kJ). The XRD traces in Fig. 2(a) reveal that the broad diffraction maxima can be obtained at the input energy of 0.1 and 0.2 kJ. With further increasing input energy up to 0.5 kJ, one can find the sharp diffraction intensity indicating formation of the crystalline phases after EDS. Fig. 2(b) presents DSC traces of the compacts with 3 mm in diameter. The onset temperatures of the glass transition and crystallization are clearly detectable from the compacts, applied at the low input energy (0.1 and 0.2 kJ) during EDS. Furthermore, one can find that the onset temperatures of the glass transition and crystallization and heat release for the exothermic reactions from the compacts are more or less identical to those from the gas-atomized powders shown in Fig. 1(b). On the contrary, there is no exothermic reaction from the compacts fabricated at high input energy (0.3–0.5 kJ) during EDS. Based on these results, it is possible to conclude that the amorphous structure is

decomposed into the crystalline phases when the high input energy more than 0.3 kJ is applied on the sample.

The SEM micrograph of the amorphous $Cu_{54}Zr_{22}Ti_{18}Ni_{6}$ compacts applied at the input energy of 0.2 kJ [Fig. 2(c)] presents that the pores are homogeneously distributed throughout the sample. The volume fraction of the pores is ~45 vol.% approximately. Furthermore, the SEM micrographs reveals that average pore size and size distribution are measured to be about 65 μm and 38–82 μm, respectively. The inset SEM micrograph obtained at high magnification reveals the formation of necks between the amorphous $Cu_{54}Zr_{22}Ti_{18}Ni_{6}$ powders. The SEM micrograph of the amorphous $Cu_{54}Zr_{22}Ti_{18}Ni_{6}$ compacts applied at the input energy of 0.3 kJ [Fig. 2(d)] reveals the formation of the homogenous pores similar to Fig. 2(c). However, one can find that the volume fraction of the pores, average pore size and size distribution significantly decrease down to ~20 vol.%, 42 μm and 18–53 μm respectively. The detailed microstructure of the amorphous $Cu_{54}Zr_{22}Ti_{18}Ni_{6}$ compacts applied at the input energy of 0.3 kJ in the inset SEM in Fig. 2(d) indicates that most $Cu_{54}Zr_{22}Ti_{18}Ni_{6}$ powders are interconnected to decrease the pore size. The SEM micrograph the amorphous $Cu_{54}Zr_{22}Ti_{18}Ni_{6}$ compacts applied at the input energy of 0.5 kJ [Fig. 2(e)] shows formation of the dense solid with few pores. Furthermore, the inset SEM image in Fig. 2(e) reveals the typical dendritic microstructure on the dense solid area indicating the crystallization of the amorphous $Cu_{54}Zr_{22}Ti_{18}Ni_{6}$ powders during EDS. Therefore, it is possible to consider that the porous $Cu_{54}Zr_{22}Ti_{18}Ni_{6}$ metallic glass compacts with 3 mm in diameter can be successfully fabricated using EDS only when the input energy is 0.1 and 0.2 kJ.

In order to clarify the effect of the electrical input energy on the formation of the porous $Cu_{54}Zr_{22}Ti_{18}Ni_{6}$ metallic glass compacts, we have performed EDS with the different diameter (4 mm in diameter). Fig. 3 shows XRD traces (a), DSC traces (b) and SEM micrographs [(c)–(e)] with inset SEM micrographs obtained at higher magnification of the porous $Cu_{54}Zr_{22}Ti_{18}Ni_{6}$ metallic glass compacts with 4 mm in diameter fabricated using EDS with different electrical input energies (0.3–0.7 kJ). The XRD traces in Fig. 3(a) reveal that the broad diffraction maxima are visible only when

the input energy is applied at 0.3 and 0.5 kJ. The DSC traces in Fig. 3(b) show that the exothermic reactions occur when the porous compacts have fabricated at the input energy of 0.3 and 0.5 kJ. Moreover, it is possible to find that onset temperatures of the glass transition and crystallization and heat release for the exothermic reactions from the compacts are more or less identical to those from the gas-atomized powders. This indicates that there is no clear change on the thermal stability of the amorphous powders even after EDS with input energy of 0.3 and 0.5 kJ. As similar to the porous $Cu_{54}Zr_{22}Ti_{18}Ni_6$ metallic glass compacts with 3 mm in diameter, there is a tendency to decompose the amorphous phase into crystalline phases with increasing the input energy. However, it is worth to note that an increase of the size of the porous $Cu_{54}Zr_{22}Ti_{18}Ni_6$ metallic glass compact is necessary to apply the high input energy during EDS.

The SEM micrograph in Fig. 3(c) reveals that the pores homogenously form with volume fraction of ~50 vol.%, average pore size of 87 μm and size distribution of 30–100 μm. The inset SEM micrograph in Fig. 3(c) clearly shows the formation of the necks between the amorphous $Cu_{54}Zr_{22}Ti_{18}Ni_6$ powders. With further increasing the input energy, the volume fraction of the pores decreases down to ~30 vol.% as shown in Fig. 3(d). Analysis of SEM images reveals that average pore size and size distribution are estimated to be 52 μm and 20–75 μm, respectively. By comparing the results between 3 mm and 4 mm compacts, one can find that pore size and size distribution decrease with increasing input energy. Furthermore, the inset SEM micrograph in Fig. 3(d) presents that the crystallization occurs at the surface areas of the amorphous powders. This implies that the surface of the amorphous powders can be a route to pass through the electrical input energy during EDS. With further increase of the input energy up to 0.7 kJ as shown in Fig. 3(e), one can find very interesting microstructure. The SEM micrograph in Fig. 3(e) reveals the formation of pore-gradient structure from central to outer areas of the sample. The dense solid forms at the central area of the sample whereas the porous structure occurs at the outer area. The formation of the pore-gradient structure using EDS has been reported previously in order to improve the osseointegration of the biocompatible Ti alloys [16] and hydrogen storage quasicrystals [17]. The inset SEM micrograph in Fig. 3(e) obtained at high magnification indicates that the crystallization occurs when the input energy of 0.7 kJ is applied. Hence, it is possible to consider that the porous $Cu_{54}Zr_{22}Ti_{18}Ni_6$ metallic glass compacts with 4 mm in diameter can form when the input energy of 0.3 and 0.5 kJ is applied during EDS. By comparing the porous $Cu_{54}Zr_{22}Ti_{18}Ni_6$ metallic glass compacts fabricated using EDS at various conditions, e.g. different applied input energy and diameters, it is possible to effectively control the volume fraction and distribution of the pores. In general, the high input energy during EDS causes the crystallization of the amorphous powders. Furthermore, the crystallization occurs at the surface of the powders where the applied electrical energy passes. Therefore, it is possible to consider that the EDS with the optimized processing conditions can

be one of the effective ways to fabricate the porous metallic glass compacts.

4. Summary

Electro-discharge sintering was used to fabricate the porous $Cu_{54}Zr_{22}Ti_{18}Ni_6$ metallic glass compacts under the various processing conditions such as the applied input energy and diameter of compacts. When the porous $Cu_{54}Zr_{22}Ti_{18}Ni_6$ metallic glass compacts with 3 mm in diameter were prepared by EDS, the volume fraction of the homogeneously distributed pores can be controlled from 45 to 20 vol.% by varying the input energy from 0.1 to 0.2 kJ. In contrast, the volume fraction of the pores from 50 to 30 vol.% in the porous $Cu_{54}Zr_{22}Ti_{18}Ni_6$ metallic glass compacts with 4 mm in diameter was controlled with increasing the input energy from 0.3 to 0.5 kJ during EDS. However, the porous $Cu_{54}Zr_{22}Ti_{18}Ni_6$ metallic glass compacts with both 3 and 4 mm in diameter were decomposed into crystalline phases when the applied input energy during EDS is high. Therefore, it is possible to introduce EDS as one of the effective processing routes to produce the porous metallic glass compacts with the optimized processing conditions.

References

[1] A. Inoue, Acta Mater. 48 (2000) 279.
[2] W.L. Johnson, Mater. Res. Bull. 24 (1999) 42.
[3] C.P. Kim, R. Bush, A. Masuhr, H. Choi-Yim, W.L. Johnson, Appl. Phys. Lett. 79 (2001) 1456.
[4] C. Fan, R.T. Ott, T.C. Hugnagel, Appl. Phys. Lett. 81 (2002) 1020.
[5] A.H. Brothers, D.C. Dunand, Appl. Phys. Lett. 84 (2004) 1108.
[6] J. Schroers, C. Veazey, M.D. Demetriou, W.L. Johnson, J. Appl. Phys. 96 (2004) 7723.
[7] T. Wada, A. Inoue, A.L. Greer, Appl. Phys. Lett. 86 (2005) 251907.
[8] A.H. Brothers, D.C. Dunand, Q. Zheng, J. Xu, J. Appl. Phys. 102 (2007) 023508.
[9] G. Xie, W. Zhang, D.V. Louzguine-Luzgin, H. Kimura, A. Inoue, Scripta Mater. 55 (2006) 687.
[10] J. Schroers, C. Veazey, W.L. Johnson, Appl. Phys. Lett. 82 (2003) 370.
[11] T. Wada, A. Inoue, Mater. Trans. 45 (2004) 2761.
[12] M.H. Lee, D.J. Sordelet, Appl. Phys. Lett. 89 (2006) 89.
[13] W.H. Lee, C.Y. Hyun, J. Mater. Process. Technol. 189 (2007) 219.
[14] Y.B. An, W.H. Lee, Mater. Chem. Phys. 95 (2006) 242.
[15] Y.W. Cheon, Y.J. Jo, C.M. Lee, H.S. Jang, K.B. Kim, W.H. Lee, Mater. Sci. Eng. A 467 (2007) 89.
[16] G.A. Song, J.S. Shin, T.J. Kang, H.S. Choi, J.K. Lee, M.H. Lee, T.S. Kim, W.H. Lee, K.B. Kim, Surf. Rev. Lett. 17 (2010) 245.
[17] G.A. Song, J.S. Shin, T.J. Kang, H.S. Choi, J.K. Lee, M.H. Lee, T.S. Kim, E. Fleury, F. Prima, W.H. Lee, K.B. Kim, J. Alloys and Comps. 504S (2010) S302.